Implementation Limitations of STANAG 1008 Design Constraints for Pulsed Loads

George J. Tsekouras[a], Fotis D. Kanellos[b], John M. Prousalidis[c] and Ioannis K. Hatzilau[a]

[a] *Hellenic Naval Academy, Department of Electrical Engineering and Computer Science, Terma Hatzikiriaku, 18539, Piraeus, Greece*
[b] *Technical University of Crete, Production Engineering & Management Department, Chania, 73100, Greece*
[c] *National Technical University of Athens, School of Naval Architecture and Marine Engineering, 9, Iroon Polytecheniou Street, 157 80, Zografou Campus, Athens, Greece*

Abstract. Crucial power quality problems in ship electric power systems, known as "voltage/frequency modulation", are usually caused by specific type of loads known as "pulsed loads". Pulsed loads require regularly or randomly repeated high power consumption in short time intervals. NATO standard, STANAG 1008, imposes two design inequalities involving the power factor of the pulsed load and the ratio between the apparent power of the pulsed load and the full rated apparent power of the supply at the occurrence of the pulse. If these two inequalities are satisfied for a low voltage ship service power supply system, the voltage and frequency modulation will not exceed 2% and 0,5%, respectively. However, no well-based theoretical analysis of the phenomenon is used. The mathematical analysis of voltage/frequency phenomenon was presented in a series of two companion past papers proving that the phenomenon is depends on several parameters such as pulsed load period and duty cycle, the technical characteristics of the generators and their frequency and voltage controllers, the technical characteristics of the cable between the pulsed load and the generator etc. In this paper, the impact of the aforementioned parameters to STANAG 1008 design constraints for voltage and frequency modulation will be examined based on the theoretical analysis already developed by the authors. The effects of the respective parameters on STANAG 1008 pulsed load limit curves are presented and commented highlighting some of the issues to be addressed by future standards.

Keywords: Ship electric power system, STANAG 1008, pulsed loads, voltage and frequency modulation, modeling.
PACS: 84.70.+p

INTRODUCTION

In recent years Power Supply Quality (PSQ) for ship power systems has become a significant issue as the equipment installed on board is increasingly electrified. One of the most critical PSQ problems is "voltage and frequency modulation". Generally, "modulation" is defined as "voltage and frequency periodic or quasi-periodic variations such as might be caused by regularly or randomly repeated loading with frequency less than nominal" [1-3]. Pulsed loads provoke modulation, as they require high power for a very short time interval (in the order of a few seconds or even up to some milliseconds). This operation is often repeated on a regular or almost regular basis introducing a periodicity on the entire phenomenon.

The primary effects of pulse loading have been already studied in the context of voltage flicker, dynamic and transient stability, excitation of torsional frequencies in generators etc according to previous experience from continental power systems [4]. Pulse loading may also affect the operation of several subsystems of the ship such as radarscopes, communication and navigation equipment etc.

Voltage and frequency modulations are calculated as the difference between maximum and minimum values expressed as a percentage of the double of the nominal value as shown in (1) and (2):

$$M_V = \frac{V_{\max} - V_{\min}}{2V_n} \tag{1}$$

$$M_f = \frac{f_{\max} - f_{\min}}{2f_n} \tag{2}$$

Voltages in (1) may be used in rms, peak or mean values.

In Fig. 1, voltage and frequency modulation caused by a rectangular pulsed load is shown.

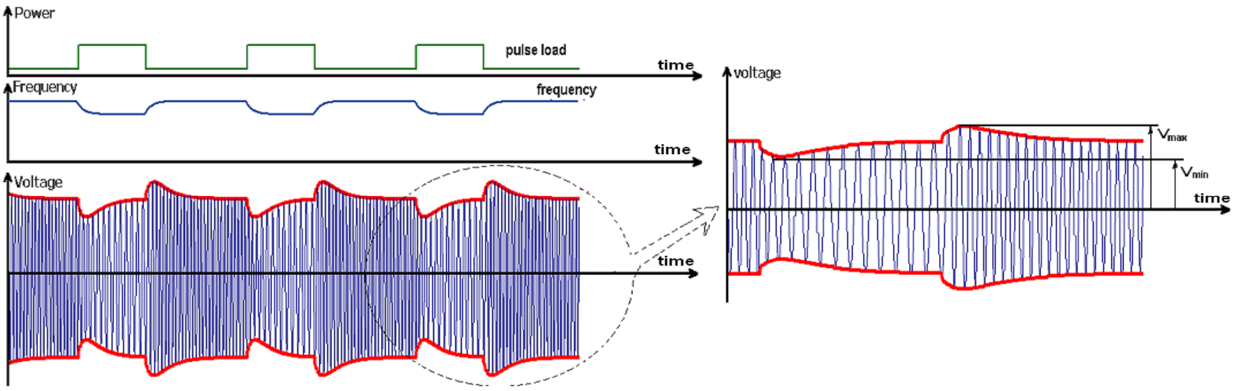

FIGURE 1. Frequency and voltage modulation caused by a rectangular pulsed load.

Up to now, few standards have dealt with this issue and have released relevant rules. Especially, in IEEE-45 the respective parameters have not been quantified [1], while USA-MIL-1399 [3] is overlapped with STANAG-1008 [2]. The following analysis will be based on STANAG 1008 (edition 9) [2], which is the NATO naval standard dealing with PSQ issues. It sets the limits of voltage and frequency modulation for the low voltage shipboard electrical power systems (440 V, 115 V, 60 Hz, 400 Hz) to 2% and 0.5%, respectively. STANAG 1008 deals only with the Ship Service Power Supply System excluding ship electric propulsion systems.

According to the design constraints of STANAG 1008 [8: Annex B § 9.d], in order voltage and frequency modulation not to exceed the aforementioned limits, reactive and active power of the pulsed load should satisfy the following inequalities:

Voltage modulation: $\Delta Q < 0.065 \cdot S_S$ (3)

Frequency modulation: $\Delta P < 0.25 \cdot S_S$ (4)

where ΔP and ΔQ are the active and the reactive power of the pulsed load respectively, S_S is the full rated apparent power of the supply at the occurrence of the pulsed load. Considering the apparent power of the pulsed load *ΔS* and the power factor of the pulsed load $\cos\phi$, the inequalities (3) and (4) can be written as:

$$\text{Voltage modulation: } \cos\phi > \sqrt{1-\left(a\cdot\frac{1}{\Delta S}\right)^2} \;:\; a = 0.065 \quad (5)$$

$$\text{Frequency modulation: } \Delta S\cdot\cos\phi < \beta \;:\; \beta = 0.25 \quad (6)$$

where *α* and *β* are the two parameters affecting the dimension of acceptable and unacceptable areas of operation. STANAG *α, β* parameters are fixed at 0.25 and 0.065, respectively. The respective graphical representation of inequalities (5), (6) is shown in Fig.2.

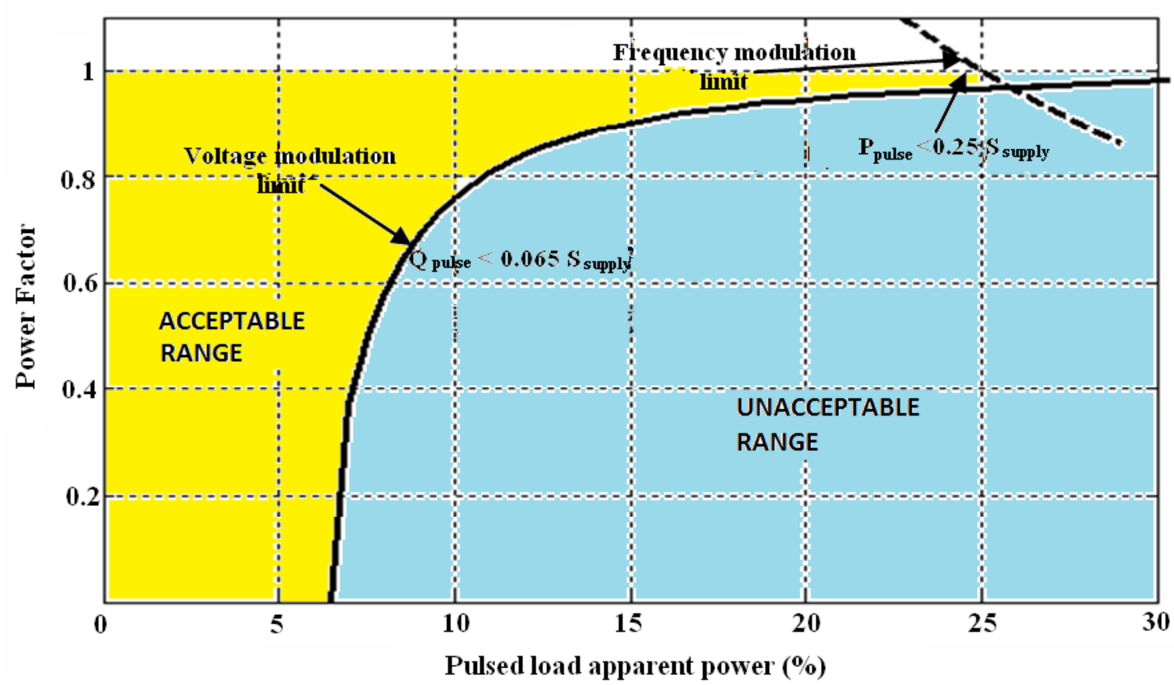

FIGURE 2. Limit curves for pulsed load operation according inequalities (5) and (6), where the acceptable and unacceptable range of pulsed load installed capacity is highlighted.

In previous papers of the authors [5-7], the electric power system of conventional ship and of All-Electric Ship has been examined proving that STANAG 1008 guideline seems to be a method leading to a rather rough estimation of pulsed loads limits, as it considers only the pulsed load relative apparent power *ΔS* and the power factor of the pulsed load $\cos\phi$. However, additional parameters such as the pulse load period and duty cycle, the time-profile and the point of the connection of the pulsed load, the technical characteristics of the generators (like sub-transient reactance, intertia) and their associated frequency and voltage controllers (like governor and automatic voltage regulator (AVR) gains etc), the loading factor of the generator at the time of the pulsed load occurrence, the equivalent length of the cable between the pulsed load and the generator etc, should be taken into account

Later, in a series of two companion papers [8-9] the theoretical analysis of the frequency and voltage modulation has been presented for a simplified ship power system respectively leading to more complex inequalities including all the above mentioned affecting parameters.

In this paper, the STANAG 1008 design constraints for voltage and frequency modulation will be examined based on the respective theoretical analysis of ship's simplified power system [8-9]. Emphasis will be placed on the effects of the respective parameters on the pulsed load limit curves of STANAG 1008 and the respective deviations caused by the variation of the parameters affecting voltage/frequency modulation will be demonstrated.

THEORETICAL ANALYSIS OF FREQUENCY & VOLTAGE MODULATION IN A SIMPLIFIED SHIP'S ELECTRIC POWER SYSTEM

Simplified Electrical Circuit of Ship Power System

The electric power system of a ship is considered as simplified as possible, as shown in Fig. 3 and proposed in [5]. The proposed simplified configuration can lead to the equivalent model of a conventional ship or an All Electric Ship. According to this approach, the bulk power produced by the equivalent synchronous generator is transferred to the load via a major electrical path with complex impedance $R+j{\cdot}X_C$. Automatic voltage and frequency regulators control the AC voltage and its frequency, respectively.

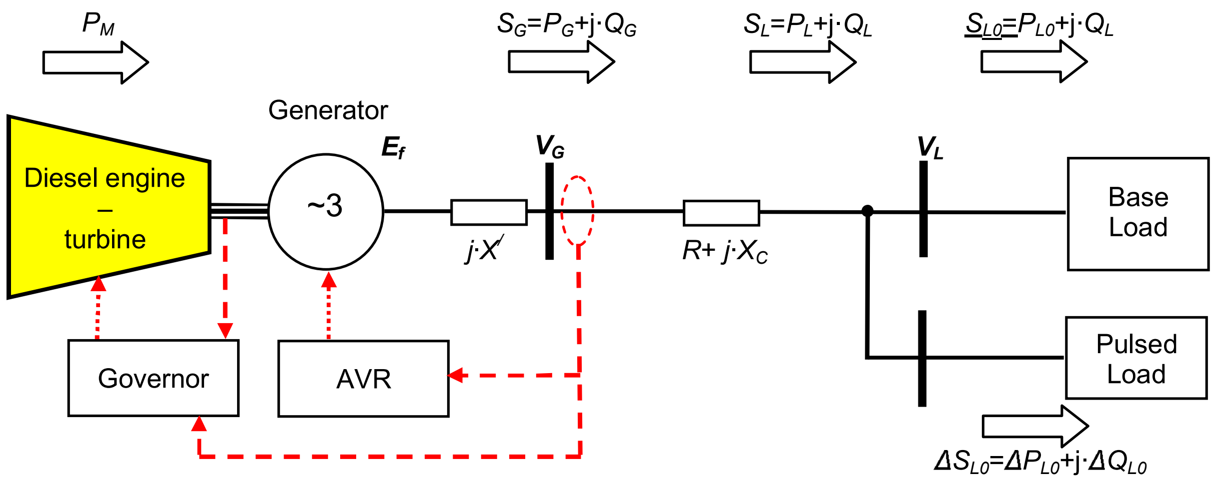

FIGURE 3. Equivalent topology of a ship electric power system.

For the following analysis the electric and mechanical parameters with the respective measurement units used, are listed next:

- E_F is the generator excitation voltage (V [volts] or p.u. [per unit]),
- V_G is the voltage at the generator ends (V or p.u.),
- V_L is the voltage at the load connection point (V or p.u.),
- E_{F0} is the generator excitation voltage (p.u.) before the occurrence of the pulsed load,
- V_{G0} is the voltage at the generator ends (p.u.) before the occurrence of the pulsed load,
- V_{L0} is the voltage at the load connection point (p.u.) before the occurrence of the pulsed load,
- T_M is the accelerating mechanical torque on generator shaft (Nm),
- T_G is the electromechanical torque on generator gap (Nm),
- P_M is the accelerating mechanical power on generator shaft (W or p.u.),

- S_G, P_G, Q_G are the apparent, the active and the reactive power produced by the generator respectively (VA or p.u., W or p.u., var or p.u.),
- S_S is the full rated apparent power of the supply at the occurrence of the pulsed load, which is the nominal base apparent power of the electric power system (VA),
- X' is the equivalent sub-transient reactance of the generator (Ω or p.u.),
- R, X_C are the equivalent resistance and the equivalent reactance of the cables between generator output and load bus respectively (Ω or p.u., Ω or p.u.),
- S_L, P_L, Q_L are the apparent, the active and the reactive power of the system load respectively (VA or p.u., W or p.u., var or p.u.),
- S_{L0}, P_{L0}, Q_{L0} are the apparent, the active and the reactive power of the system base load (without the pulsed load) respectively (VA or p.u., W or p.u., var or p.u.),
- ΔS, ΔP, ΔQ are the apparent, the active and the reactive power of the system pulsed load respectively (VA or p.u., W or p.u., var or p.u.),
- ω, f are the ship electric power system cyclic frequency and the respective frequency (rad/s or p.u., Hz or p.u.),
- ω_0, f_0 is the ship electric power system base cyclic frequency and the respective base frequency (rad/s or p.u., Hz or p.u.),
- Δf is the frequency deviation from its nominal value and is equal to $1\text{-}f$ (p.u.),
- J is the generator rotor inertia constant (kg·m^2),
- J' is the generator rotor inertia constant (s), which is equal to $J \cdot \omega_0^2 / S_S$,
- T is the pulsed load period (s),
- dc is the pulsed load duty cycle (-),
- $\cos\varphi$ is the pulsed load power factor (-),
- I_L, I_{Ld}, I_{Lq} are the system load current and the respective d-axis, q-axis components (A or p.u.),
- R_f, K_f are the frequency droop and the integral gain of the frequency regulator,
- K, K_V are the proportional and the integral gain of automatic voltage regulator respectively,
- $M_f^{\lim}$ is the frequency modulation limit (-),
- $M_V^{\lim}$ is the voltage modulation limit (-).

The supplied load consists of a base load (including electric propulsion in the case of All Electric Ship) and a pulsed load. A typical pulsed load profile as that shown in Fig. 4a is used for the analysis that follows. System pulsed load is modeled by the following expressions:

$$\Delta S(t) = \Delta S \cdot \sum_{n=0}^{\infty} \left[u(t - n \cdot T) - u(t - (n + dc) \cdot T) \right] \tag{7}$$

$$\Rightarrow \Delta P(t) = \Delta S \cdot \cos\varphi \cdot \sum_{n=0}^{\infty} \left[u(t - n \cdot T) - u(t - (n + dc) \cdot T) \right] \tag{8}$$

where $u(t)$ is the unit step-function.

Constant power load modeling approach is fairly accurate for the examined range of frequency and voltage deviation, provided that that loads in modern ship configurations are often interfaced with the grid via power electronic converters, which provide fast dynamic reactions. So the respective profile of the total load demand is presented in Fig. 4b.

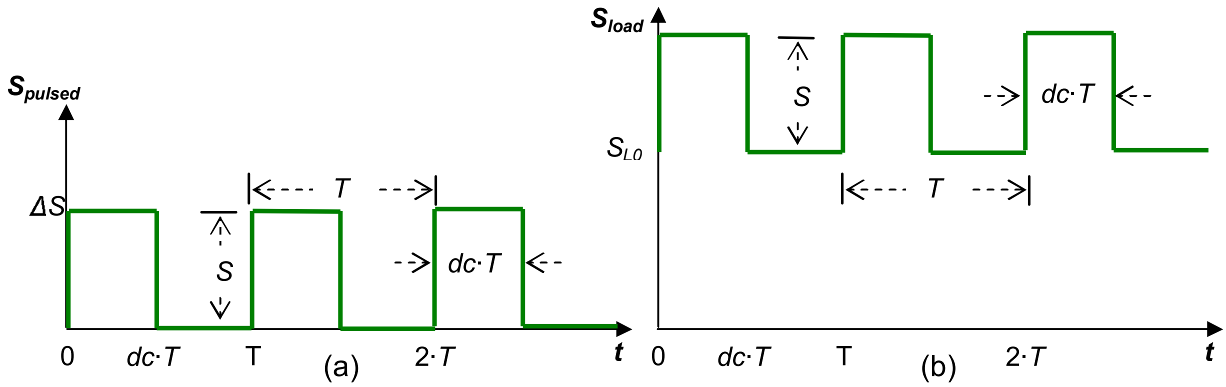

FIGURE 4. a) Pulsed load typical profile, b) total load typical profile.

Frequency Modulation Estimation

Here, the mathematical base of frequency modulation in the presence of pulsed load is presented. The detailed mathematical nalysis can be found in [8].

If friction losses are neglected, then the motion equation of the generator rotor is:

$$J \cdot \frac{d\omega}{dt} = T_M - T_G \tag{9}$$

Taking into consideration that P_M is the accelerating mechanical power, P_G the active power produced by the generator, ω is the rotor rotating speed, which is equal to frequency f in p.u., and Δf=1-f, equation (8) can be rewritten:

$$J' \cdot f \cdot \frac{d\Delta \mathrm{f}}{\mathrm{dt}} = \Delta P_G - \Delta P_M\,(p.u.) \tag{10}$$

If both primary and secondary frequency adjustment is taken into account, the frequency droop equation of the generator is:

$$\Delta P_M = R_f \cdot \Delta f + K_f \cdot \int_o^t \Delta f \cdot d\tau \tag{11}$$

Where, R_f is the frequency droop of the combination of the generator and its associated speed governor, K_{fi} the integral gain of the speed controller.

Assuming that frequency is close to its nominal value ($f \approx 1$ p.u.) and taking into consideration the set of equations (8), (10) and (11) the following equation is obtained:

$$J' \cdot \frac{d\Delta f}{dt} = \Delta S \cdot \cos\varphi \cdot \sum_{n=0}^{\infty} \left[u(t - n \cdot T) - u(t - (n + dc) \cdot T) \right] - R_f \cdot \Delta f - K_f \cdot \int_o^t \Delta f \cdot d\tau \tag{12}$$

If

$$R_f^2 > 4 \cdot J' \cdot K_f \tag{13}$$

then by applying Laplace and inverse Laplace transformation to equation (12) frequency in time domain is equal to:

$$\Delta f(t)=\frac{\Delta S\cdot\cos\phi}{J'\cdot(p_2-p_1)}\cdot\sum_{n=0}^{\infty}\left[\begin{array}{l}\left(e^{-p_1(t-nT)}-e^{-p_2(t-nT)}\right)\cdot u(t-nT)\\-\left(e^{-p_1(t-(n+dc)\cdot T)}-e^{-p_2(t-(n+dc)\cdot T)}\right)\cdot u(t-(n+dc)\cdot T)\end{array}\right] \tag{14}$$

Where

$$p_1=\frac{R_f-\sqrt{R_f^2-4\cdot J'\cdot K_f}}{2\cdot J'}\qquad p_2=\frac{R_f+\sqrt{R_f^2-4\cdot J'\cdot K_f}}{2\cdot J'} \tag{15}$$

According to (2) and taking into account the frequency function of eq. (14), frequency modulation becomes:

$$M_{\mathrm{f}}=\frac{f_{\max}-f_{\min}}{2f_n}=\frac{\Delta\mathrm{S}\cdot\cos\phi\cdot c}{2\cdot f_n\cdot\sqrt{R_f^2-4\cdot J'\cdot K_f}} \tag{16}$$

with the parameter *c* calculated as follows:

$$c=c^{/}\left(p_1,dc,T,t_{\max 1},t^{/}_{\max 2}\right)-c^{/}\left(p_2,dc,T,t_{\max 1},t^{/}_{\max 2}\right) \tag{17}$$

where,

$$t_{\max 1}=\max\left(\frac{1}{p_2-p_1}\cdot\ln\left[\frac{p_2}{p_1}\cdot\frac{\left(e^{p_2 dcT}-1\right)}{\left(e^{p_1 dcT}-1\right)}\cdot\frac{\left(e^{p_1 T}-1\right)}{\left(e^{p_2 T}-1\right)}\right],\ 0\right) \tag{18}$$

$$t^{/}_{\max 2}=\min\left(\frac{1}{p_2-p_1}\cdot\ln\left[\frac{p_2}{p_1}\cdot\frac{\left(e^{p_2 T}-e^{p_2 dcT}\right)}{\left(e^{p_1 T}-e^{p_1 dcT}\right)}\cdot\frac{\left(e^{p_1 T}-1\right)}{\left(e^{p_2 T}-1\right)}\right];dc\cdot T\right) \tag{19}$$

$$c^{/}\left(p,dc,T,t_{\max 1},t^{/}_{\max 2}\right)=\frac{\left(e^{pdcT}-1\right)\cdot e^{-p\cdot t_{\max 1}}+\left(e^{pT}-e^{pdcT}\right)\cdot e^{-p\cdot t^{/}_{\max 2}}-e^{pT}+e^{pdcT}}{e^{pT}-1} \tag{20}$$

Taking into consideration STANAG-1008 constraint for frequency modulation, (M_f should be smaller than $M_f^{\lim}$ = 0.5%), then the following inequality is obtained:

$$\Delta S\cdot\cos\varphi<\frac{2\cdot M_f^{\lim}\cdot f_n\cdot J'\cdot(p_2-p_1)}{c} \tag{21}$$

Inequality (21) defines a parabolic curve on the *S-cosφ* plane, as it is also foreseen by STANAG-1008 (as shown in Fig. 2 and defined by inequality (4)) involving several parameters of ship electric power system model such as *dc*, *T*, R_f, *J'*, K_f which must be taken into account during the design of the electric power system. Moreover, it appears that the *S-cosφ* limitation curve for frequency deviation is not unique as assumed in standards like STANAG-1008, but it depends on the system model parameters mentioned above. Inequality (21) has been developed within time interval $t \in [0,\infty)$, while standards, like STANAG-1008, do not define the respective study time period of the frequency modulation.

R_f should not lie into the region defined by $R_f^2=4\cdot J'\cdot K_f$ and $R_f^2<4\cdot J'\cdot K_f$ as it might provoke significant frequency oscillations.

In general the respective upper limit for frequency modulation can be expressed by a general function of the following form for this simplified ship power system:

$$F_f(T, dc, J', K_f, R_f, \Delta S, \cos\varphi) \le M_f^{\lim} \tag{22}$$

Voltage Modulation Estimation

Here, the mathematical basis for the estimation of voltage modulation caused by pulsed loads is presented. The detailed mathematical analysis can be found in [9].

More specifically the electric behavior of the system shown in Fig. 3 is similar to the behavior of an RL circuit, where the RL circuit consists of the equivalent sub-transient reactance of the generator X', the equivalent reactance X_C of the cables between generator output and load bus and the equivalent resistance R. The voltages at the ends of the RL branch, namely, the electromagnetic force E_F of synchronous generator and the load voltage V_L, are related with the current flowing through it by the following set of differential equations (all AC quantities are expressed to a rotating reference frame attached to voltage, V_L).

$$E_{Fd} = V_{Ld} + R\cdot I_{Ld} - \left(X' + X_C\right)\cdot I_{Lq} + \frac{X' + X_C}{\omega_0}\cdot\frac{dI_{Ld}}{dt} \tag{23}$$

$$E_{Fq} = \underbrace{V_{Lq}}_{0} + R\cdot I_{Lq} + \left(X' + X_C\right)\cdot I_{Ld} + \frac{X' + X_C}{\omega_0}\cdot\frac{dI_{Lq}}{dt} \tag{24}$$

It is noted that the generator saturation has been ignored in this study.

The respective vector diagram is presented in Fig. 5, where phase angle θ is the load current phase angle with respect to load voltage vector V_L.

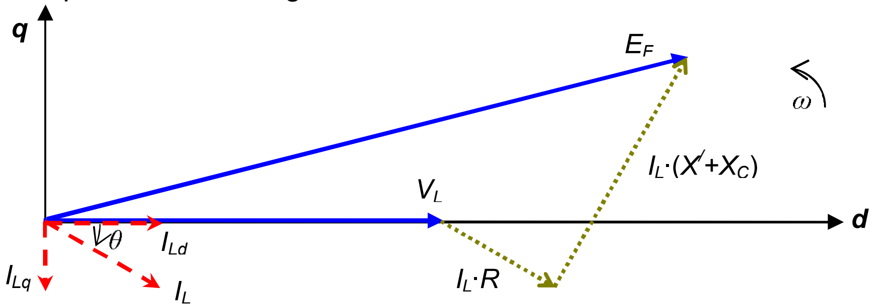

FIGURE 5. Vector diagram of simplified electrical circuit of ship power system.

For the operating conditions of the ship electric system studied in this paper, the so-called induction voltage terms (including current derivatives) in equations (23) and (24) can be neglected without affecting significantly the accuracy of the results [10, 11] and the following set of equations is formed:

$$E_{Fd} = V_{Ld} + R \cdot I_{Ld} - \left(X^{/} + X_C\right) \cdot I_{Lq} \tag{25}$$

$$E_{Fq} = R \cdot I_{Lq} + \left(X^{/} + X_C\right) \cdot I_{Ld} \tag{26}$$

The electromagnetic force E_F of synchronous generator is adjusted by the Automatic Voltage Regulator (AVR). For simplification purposes and without loss of generalization, a simple proportional – integral (PI) controller is assumed, while the generator bus is considered as the voltage control point. Thus, AVR can be modeled as following:

$$E_f = E_{f0} + K \cdot \Delta V_G + K_V \cdot \int_0^t \Delta V_G \cdot d\tau \tag{27}$$

with

$$\Delta V_G = V_{G0} - V_G = 1 - V_G \tag{28}$$

While

$$\Delta V_L = V_{L0} - V_L \tag{29}$$

$$\Delta S_L \cong S_L - S_{L0} \tag{30}$$

$$S_L = V_L \cdot I_L \text{ (root mean values)} \tag{31}$$

Where E_{F0}, V_{G0}, V_{L0}, S_{L0} are the synchronous generator electromagnetic force, the generator bus voltage, the load bus voltage and the system base load apparent power before the occurrence of the pulsed load, respectively.

Applying Laplace transformation, Taylor series expansion of E_F with respect to V_L and S_L approximated by 1st order terms and inverse Laplace transformation, load bus voltage variance is given by:

$$\Delta V_L(t) = \begin{cases} \Gamma_1 \cdot \Delta S \cdot \sum_{n=0}^{\infty} \left(u(t - n \cdot T) - \left(u(t - n \cdot T - dc \cdot T)\right)\right) \\ +\Gamma_2 \cdot \Delta S \cdot \sum_{n=0}^{\infty} \left(e^{-\gamma \cdot (t - n \cdot T)} \cdot u(t - n \cdot T) - e^{-\gamma (t - n \cdot T - dc \cdot T)} \cdot \left(u(t - n \cdot T - dc \cdot T)\right)\right) \end{cases} \tag{32}$$

where

$$V_{G0}^2 = 1 = V_{L0}^2 + \frac{R^2 + X_C^2}{V_{L0}^2} \cdot S_{L0}^2 + 2 \cdot (R \cdot \cos\varphi + X_C \cdot \sin\varphi) \cdot S_{L0} \tag{33}$$

$$V_{L0} = \sqrt{\frac{1 - 2 \cdot (R \cdot \cos\varphi + X_C \cdot \sin\varphi) \cdot S_{L0} + \left(\left(2 \cdot (R \cdot \cos\varphi + X_C \cdot \sin\varphi) \cdot S_{L0} - 1\right)^2 - 4 \cdot (R^2 + X_C^2) \cdot S_{L0}^2\right)^{1/2}}{2}} \tag{34}$$

$$E_{F0} = \left(V_{L0}^2 + \frac{R^2 + X^2}{V_{L0}^2} \cdot S_{L0}^2 + 2 \cdot (R \cdot \cos\varphi + X \cdot \sin\varphi) \cdot S_{L0}\right)^{1/2} \tag{35}$$

$$\mathrm{A}_1 = \frac{R\cdot\cos\varphi + X\cdot\sin\varphi + \dfrac{R^2+X^2}{V_{L0}^2}\cdot S_{L0}}{E_{f0}} \tag{36}$$

$$\mathrm{A}_2 = \frac{V_{L0} - \dfrac{R^2+X^2}{V_{L0}^3}\cdot S_{L0}^2}{E_{f0}} \tag{37}$$

$$\mathrm{B}_1 = \frac{R\cdot\cos\varphi + X_C\cdot\sin\varphi + \dfrac{R^2+X_C^2}{V_{L0}^2}\cdot S_{L0}}{V_{G0}} \tag{38}$$

$$\mathrm{B}_2 = \frac{V_{L0} - \dfrac{R^2+X_C^2}{V_{L0}^3}\cdot S_{L0}^2}{V_{G0}} \tag{39}$$

$$\Gamma_1 = \frac{\mathrm{B}_1}{\mathrm{B}_2} > 0 \tag{40}$$

$$\Gamma_2 = \frac{\mathrm{B}_2\cdot\mathrm{A}_1 - \mathrm{B}_1\cdot\mathrm{A}_2}{\mathrm{B}_2\cdot(\mathrm{A}_2+\mathrm{B}_2\cdot\mathrm{K})} > 0 \tag{41}$$

$$\gamma = \frac{\mathrm{B}_2\cdot K_V}{\mathrm{A}_2+\mathrm{B}_2\cdot\mathrm{K}} \tag{42}$$

According to (1) and taking into account the voltage variance function of eq. (32), voltage modulation becomes:

$$M_V = \frac{V_{\max}-V_{\min}}{2\cdot V_n} = \frac{\max\Delta V_L - \min\Delta V_L}{2\cdot V_n} = \frac{\Gamma_1+\Gamma_2\cdot\dfrac{2\cdot e^{\gamma\cdot T} - e^{\gamma\cdot T\cdot(1-dc)} - 1}{e^{\gamma\cdot T}-1}\cdot\Delta S}{2\cdot V_n} \tag{43}$$

Taking into consideration STANAG-1008 constraint for voltage modulation, (M_V should be smaller than $M_V^{\lim}$ = 2%), the following inequality is obtained:

$$M_V < M_V^{\lim} \tag{44}$$

If it is assumed that $R \approx 0$, $V_n \approx 1$ p.u., $E_F \approx 1$ p.u., $X \approx X_C$, $X+X_C \approx 2\cdot X$ and $1-X^2\cdot S_{L0}^2 \approx 1-X_C^2\cdot S_{L0}^2$, then (43) turns into,

$$M_V = \frac{\Delta S}{2}\cdot\left[Z_1 + Z_2\sin\varphi\right] \tag{45}$$

with

$$Z_1 = \frac{\mathrm{X}^2\cdot S_{L0}}{1-\mathrm{X}^2\cdot S_{L0}^2} + \frac{2\cdot\mathrm{X}'\cdot\mathrm{X}\cdot S_{L0}}{(K+1)\cdot(1-\mathrm{X}^2\cdot S_{L0}^2)^2}\cdot\frac{2\cdot e^{\gamma\cdot T} - e^{\gamma\cdot T\cdot(1-dc)} - 1}{e^{\gamma\cdot T}-1} \tag{46}$$

$$Z_2 = \frac{X}{1 - X^2 \cdot S_{L0}^2} + \frac{X' \cdot (1 + X^2 \cdot S_{L0}^2)}{(K+1) \cdot (1 - X^2 \cdot S_{L0}^2)^2} \cdot \frac{2 \cdot e^{\gamma \cdot T} - e^{\gamma \cdot T \cdot (1-dc)} - 1}{e^{\gamma \cdot T} - 1} \tag{47}$$

Then the following inequality is obtained:

$$\cos\varphi > \sqrt{1 - \left(\frac{Z_1}{Z_2}\right)^2 + \frac{4 \cdot M_V^{\lim} \cdot Z_1}{Z_2^2} \cdot \frac{1}{\Delta S} - \frac{4 \cdot \left(M_V^{\lim}\right)^2}{Z_2^2} \cdot \frac{1}{\Delta S^2}} \tag{48}$$

Considering that the products $X^2 \cdot S_{L0}^2$, $X_C^2 \cdot S_{L0}^2$ and $X \cdot X_C \cdot S_{L0}$ are negligible, then (48) becomes,

$$\cos\varphi > \sqrt{1 - \left(\frac{a}{\Delta S}\right)^2} \tag{49}$$

with

$$\alpha = \frac{2 \cdot M_V^{\lim}}{X + \frac{X'}{(K+1)} \cdot \frac{2 \cdot e^{\gamma \cdot T} - e^{\gamma \cdot T \cdot (1-dc)} - 1}{e^{\gamma \cdot T} - 1}} \tag{50}$$

that is of the same form with the inequality proposed in STANAG 1008 (see eq. (5)).

Inequalities (44), (48) and (49) define limitation curves on the S-cosφ plane similar to the one foreseen by STANAG-1008, ehich however, include several parameters of ship electric power system model such as *dc*, *T*, *K*, K_I, X_C, *X'*, S_{L0}. Therefore, it can be concluded that *S*-cosφ limitation curve for voltage deviation is not unique as assumed in standards like STANAG-1008, but it depends on the system model parameters mentioned above which must be taken into account during the design of the ship electric power system. Inequalities (48) and (49) have been also developed within time interval $t \in [0, \infty)$, while standards, like STANAG-1008, do not define the respective study time period of the voltage modulation.

In general the respective upper limit for voltage modulation can be expressed by a general function of the following form:

$$F_V(T, dc, X_C, R, X^{/}, K, K_I, S_{L0}, \Delta S, \cos\varphi) \le M_V^{\lim} \tag{51}$$

NUMERICAL ANALYSIS OF FREQUENCY & VOLTAGE MODULATION IN A SIMPLIFIED SHIP'S ELECTRIC POWER SYSTEM

Simplified Electrical Circuit of a S Frigate Power System

The electric power system of a Hellenic Naval's S frigate consists of 4 generators Smit/Slikkerver DG 77/48/60 with nominal line to line voltage 450 V, nominal frequency 60 Hz, nominal apparent power 937,5 kVA, nominal active power 750 kW, nominal power factor 0,80 (ind.) and direct axis transient reactance 0,225 p.u. (for base power equal to the nominal power of one generator). The load demand of the frigate is usually between 500 to 1500 kVA with a typical average load of 750 kVA approximately, which is equal to 80% of the nominal apparent power of one generator. For reliability reasons two generators operate in parallel, while the other two can be started in few seconds, if any of the two main generators is shut down or the demand load exceed a predifened limit.

For the rest of the analysis, the base voltage of the power system is 450 V and the system base apparent power is 1875 kVA (=2·937,5 kVA/generator). The respective direct axis transient reactance of the equivalent generator is obtained as 0,225 p.u. according to Millman's theorem. If the electromagnetic force, E_f , of each generator are of the same value then the equivalent E_F is also the same. The typical average load of 750 kVA corresponds to 0,4 p.u. of the system base apparent power. The generator rotor inertia constant (s) *J'* of the equivalent generator is the same with that of a single generator, with a typical value of 4 s.

Taking into consideration that the maximum voltage drop is 6% then the respective equivalent impedance of the cable can not exceed 0,15 p.u. for a typical average load of 750 kVA, and 0,075 p.u. for a maximum load of 1500 kVA. A typical value of impedance is considered of 0,0375 p.u.. It is noted that the ratio of impedance / resistance of a E1VV cable varies from 9,5 for cross-section of 1,5mm^2 to 1232 for cross-section of 300 mm^2. In this analysis, this ratio is assumed 50 corresponding to the cross-section of 10 mm^2, and the respective resistance 50 times smaller of the respective impedance, that is 0,00075 p.u..

Based on the respective theoretical analysis pulsed load period, *T,* can take any value with usual values between 1 ms to 10 s, while the duty cycle, *d.c.,* varies between 0% to 100%. The respective typical values of pulsed period and duty cycle are 1 s and 50%.

The parameters of the frequency regulator (frequency drop R_f and integral gain K_f) and automatic voltage regulator (proportional K and integral gain K_V) can be selected properly so that no operation problems occur. Respective typical values are: R_f =20, K_f = 10, K=5, K_V = 5.

Modulation Limitations for the Simplified Electrical Circuit of a S Frigate Power System: Basic Scenario

Based on the theoretical analysis the frequency modulation limit is estimated by ineq. (21) with $M_f^{\lim}$ = 0.5% (the STANAG-1008 limit) and the respective curve is presented together with the respective curves of STANAG 1008 for frequency and voltage modulation in Fig. 6. It is obvious that the unacceptable operating area due to frequency modulation increases, but large part of it is cancelled by the operating area determined by the STANAG 1008 voltage modulation (green dotted line). This means that there is an area of *S*-cosφ which is allowed by the STANAG-1008 curves, while it is not allowed by the theoretically obtained frequency modulation limit curve.

According to the analytical theoretical analysis the voltage modulation limit is estimated by ineq. (44) with $M_V^{\lim}$ = 2.0% (the STANAG-1008 limit) and the respective curve is presented together with the curves of STANAG 1008 for frequency and voltage modulation in Fig. 7. The respective unacceptable operating area due voltage modulation limit violation decreases significantly for big values of power factor (cos*φ*>0,4). While for small values of power factor (cos*φ*<0,4) the opposite behaviour occurs. This means that there is an area of *S*-cosφ which is allowed by the STANAG-1008 curves, while it is not allowed by the theoretically obtained voltage modulation limit curve.

If inequality (49) is used with $M_V^{\lim}$ = 2.0% (the STANAG-1008 limit), then Fig. 8 is obtained, where the unacceptable operating area due to voltage modulation limit violation has decreased more than the previous one for small values of power factor. However, in this case study it can not be used, as the equivalent impedance of the cables X_C is smaller than the equivalent direct axis transient reactance of the equivalent generator X', while in inequality (49) X_C>>X' is assumed .

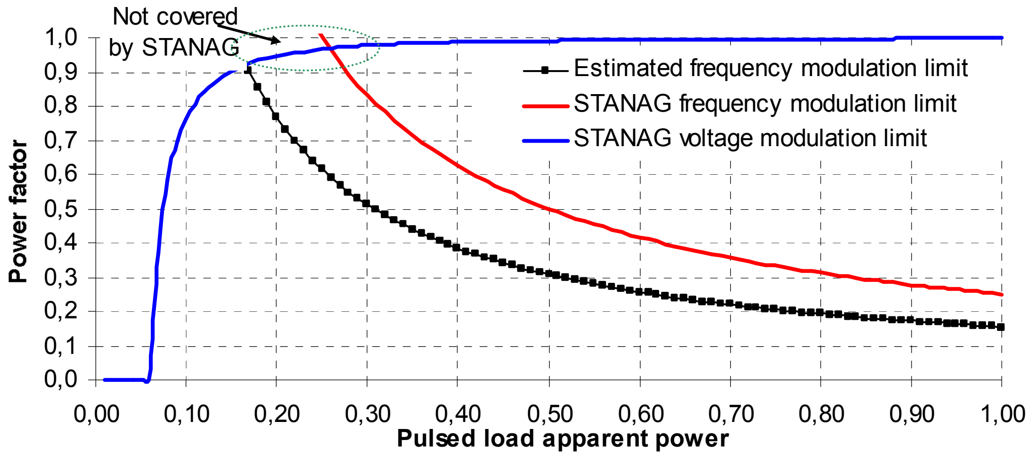

FIGURE 6. Power factor vs pulse load apparent power of the frequency modulation for the basic scenario of the simplified power system of an S frigate.

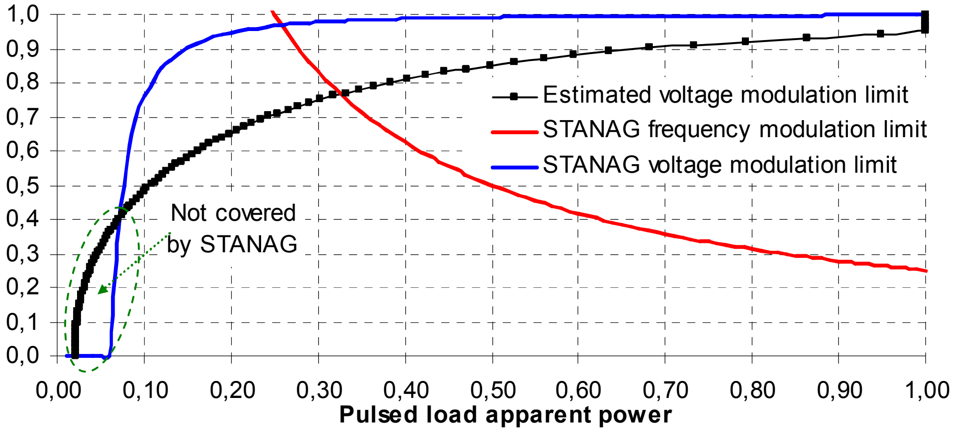

FIGURE 7. Power factor vs pulse load apparent power of the voltage modulation for the basic scenario of the simplified power system of an S frigate.

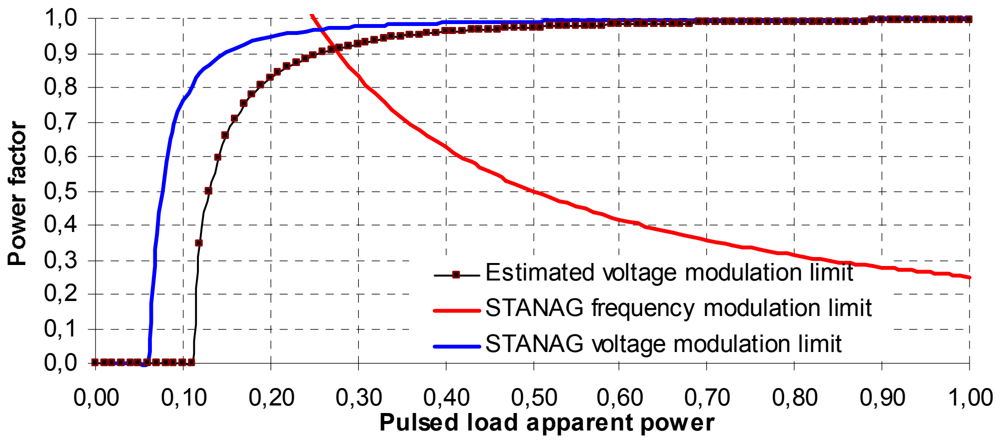

FIGURE 8. Power factor vs pulse load apparent power of the approximated voltage modulation for the basic scenario of the simplified power system of an S frigate.

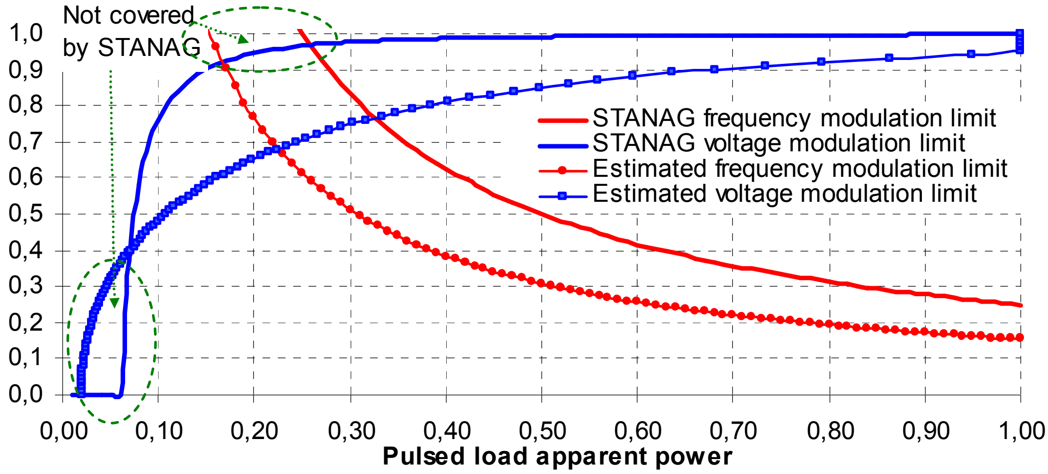

FIGURE 9. Power factor vs pulse load apparent power of the frequency modulation and the voltage modulation of the theoretical analysis for the basic scenario of the simplified power system of an S frigate.

In Fig. 9 the limit curves for the voltage and the frequency modulation are presented together with the respective ones of STANAG 1008, where the difference between the unacceptable operating areas between the theoretical analysis and STANAG 1008 becomes aparent. STANAG 1008 happens to be stricter than the theretically obtained model in case of voltage modulation, especially for power factor larger than 0.4 in case of frequency modulation is more optimistic.

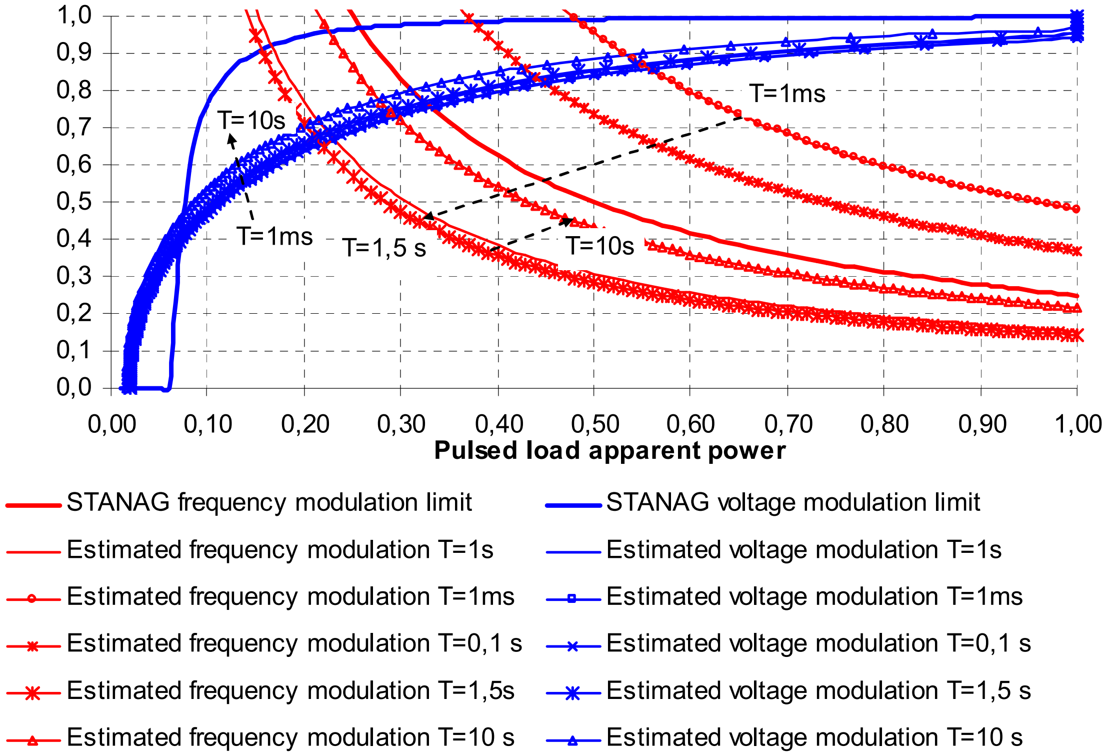

FIGURE 10. Power factor vs pulse load apparent power of the frequency modulation and the voltage modulation of the theoretical analysis for different values of the time period for the pulsed load of the simplified power system of an S frigate.

Modulation Limitations for the Simplified Electrical Circuit of a S Frigate Power System: Time Period of Pulsed Load

Pulsed load period affects both frequency and voltage modulation. The respective analysis has been developed for a range of values from 1 ms up to 10 s as following: from 1 ms up to 20 ms with a time step of 1 ms,fro 20 ms up to 100 ms with a time step of 10 ms, from 200 ms up to 2 s with a step of 100 ms, from 2 s up to 10 s with a step of 1 s.

In Fig. 10 the respective results are presented. The unacceptable operating area due to frequency modulation limit violation increases for pulsed load period less than 1,5 s, while it decreases for larger values. The theoretical curve coincides to STANAG curve for T=0,32s, approximately. The unacceptable operating area of the theoretical analysis for pulsed load period greater than 0,32s is larger than the respective one of STANAG 1008.

The unacceptable operating area due to voltage modulation increases for pulsed load period ranging from 1 ms to 10 s. However, the impact is not significant while the unacceptable operating area obtained by the theoretical analysis is smaller than the respective one of STANAG 1008; especially for power factor values greater than 0,5.

Modulation Limitations for the Simplified Electrical Circuit of a S Frigate Power System: Duty Cycle of Pulsed Load

Pulsed load duty cycle *d.c.* of affects both frequency and voltage modulation. The respective analysis has been developed for a range of values from 1% up to 99% with a step of 1%.

In Fig. 11 the respective results for pulsed load duty cycle are presented. The unacceptable operating area due to frequency modulation limit violation increases until pulsed load duty cycle becomes equal to 65% ~ 70%; while it decreases for larger values. The theoretical curve coincides to STANAG's one for *d.c.*= 20%, approximately. The unacceptable operating area as obtained by the theoretical analysis for pulsed load duty cycle greater than 20% is larger than the respective one as obtained by STANAG 1008.

The unacceptable operating area due to voltage modulation limit violation increases with pulsed load duty cycle, but the observed increse is small while the unacceptable operating area obtained by the theoretical analysis is smaller than STANAG's respective one for power factor larger than 0,5.

Modulation Limitations for the Simplified Electrical Circuit of a S Frigate Power System: Generation Rotor Inertia

Generator rotor inertia constant J' affects only frequency modulation. The values of this parameter should satisfy the following inequality according to the respective theoretical analysis (see inequality (13)):

$$R_f^2 > 4 \cdot J' \cdot K_f \Rightarrow J' < \frac{R_f^2}{4 \cdot K_f} \tag{52}$$

Taking into consideration that in the basic scenario, R_f =20, K_f = 10 Hz, then J' should be smaller than 10 s. The respective analysis has been developed for J' values ranging from 0 s up to 10 s as following: from 0 ms up to 30 ms with a step of 1 ms, from 30 ms up to 200 ms with a step of 10 ms, from 200 ms up to 9,9 s with a step of 100 ms, from 9,9 s up to 9,99 s with a step of 10 ms.

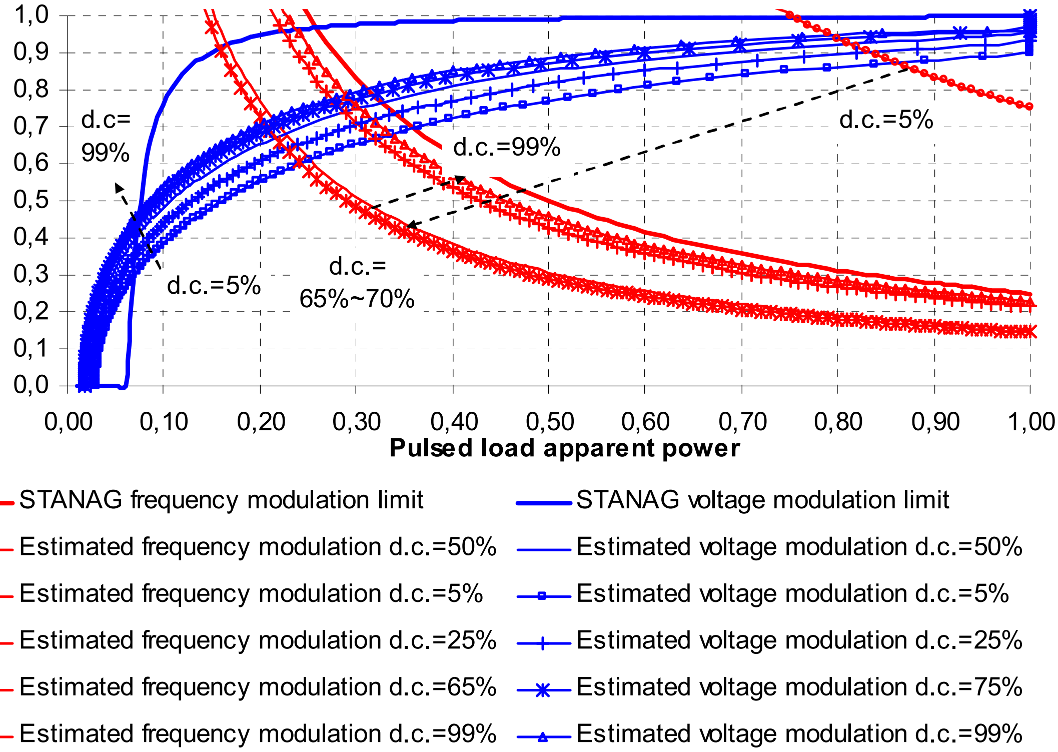

FIGURE 11. Power factor vs pulse load apparent power of the frequency modulation and the voltage modulation of the theoretical analysis for different values of the duty cycle for the pulsed load of the simplified power system of an S frigate.

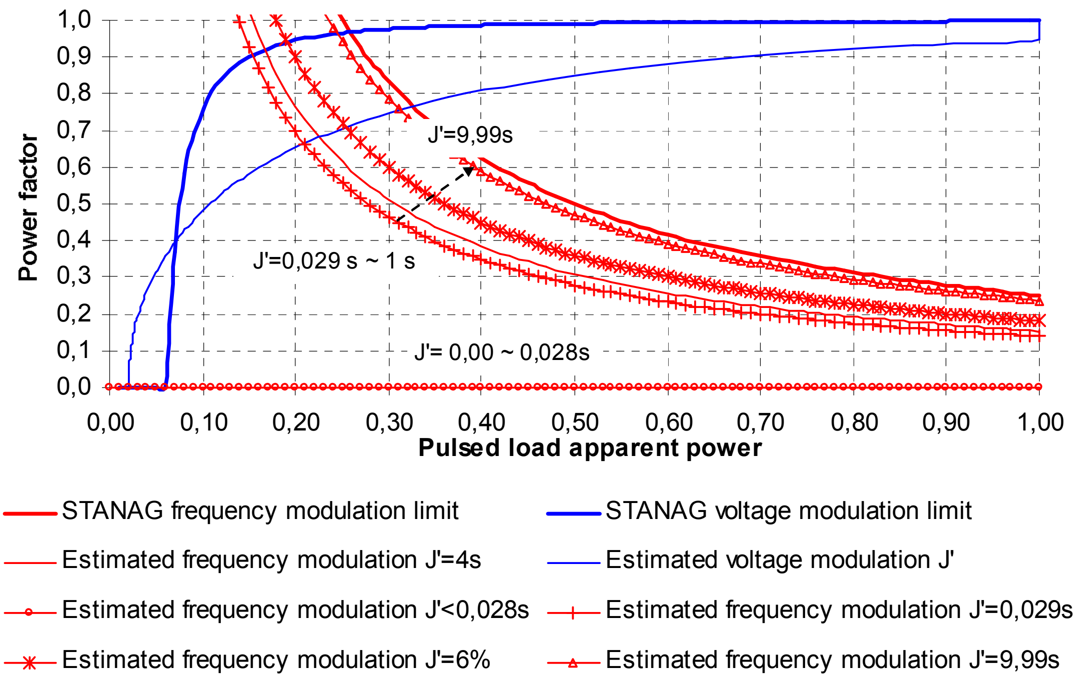

FIGURE 12. Power factor vs pulse load apparent power of the frequency modulation and the voltage modulation of the theoretical analysis for different values of the generator rotor inertia constant of the simplified power system of an S frigate (0≤J'<10 s).

In Fig. 12, the respective results considering different values of generator rotor inertia constant are presented. The unacceptable operating area due frequency modulation violation decreases in a non-linear fashion, as generator rotor inertia increases. For extremely small values (not met in practice) the respective curve becomes horizontal. The theoretically obtained limit curve tends to coincide wirth STANAG's one for large values of J/ . Values larger than 10 s lead to frequency oscillations and they should be avoided [8]. The unacceptable operating area as obtained by the theoretical analysis is larger than the respective one obtained by STANAG 1008. The effect of J/ is limited practically, as J/ can be calculated easily and it has not significant variations throughout generator life.

Modulation Limitations for the Simplified Electrical Circuit of a S Frigate Power System: Frequency Drop of Frequency Regulator

Frequency droop R_f applied to the generator frequency regulator affects only frequency modulation. The values of this parameter should satisfy the following inequality according to the respective theoretical analysis (see inequality (13)):

$$R_f^2 > 4 \cdot J' \cdot K_f \Rightarrow R_f > \sqrt{4 \cdot J' \cdot K_f} \tag{53}$$

Taking into consideration that in the basic scenario, $J' = 4$ s, $K_f = 10$ Hz , then the R_f should be larger than 12,649. The usual values of R_f lie between 20 and 100. The respective analysis has been developed for R_f ranging from 12,65 up to 150 as following: from 12,65 up to 13 with a a step of 0,05, from 13 up to 20 with a step of 1, from 20 up to 150 with a step of 5.

In Fig. 13, the respective results are presented. The unacceptable operating area due frequency modulation limit violation decreases in a nonlinear fashion as R_f increases. The theoretically obtained curve coincides to STANAG's one for R_f = 36, approximately. R_f practically should be large enough so that the respective unacceptable operation area due to frequency modulation limit violation be suppressed. However, large values of R_f can lead to significant active power generation variations even for small variations of frequency, which is not desirable for system stability reasons.

Modulation Limitations for the Simplified Electrical Circuit of a S Frigate Power System: Integral Gain of Frequency Regulator

The integral gain of generator frequency regulator affects only frequency modulation. K_f should satisfy the following inequality according to the respective theoretical analysis (see inequality (13)):

$$R_f^2 > 4 \cdot J' \cdot K_f \Rightarrow K_f < \frac{R_f^2}{4 \cdot J'} \tag{54}$$

Taking into consideration that, R_f =20 and $J' = 4$ s for the the basic scenario then K_f should be smaller than 25 Hz. It should also be positive, because, if K_f=0 then no secondary frequency is possible leading to a permanent, "steady-state", frequency error [8]. The folowing analysis has been developed for K_f ranging from 1 mHz up to 25 Hz as following: from 1 mHz up to 20 mHz with a step of 1 mHz, from 20 mHz up to 100 mHz with a step of 10 mHz, from 100 mHz up to 1 Hz with a step of 100 mHz, from 1 Hz up up to 24 Hz with a step of 1 Hz, from 24,1 Hz up to 24,9 Hz with a step of 100 mHz.

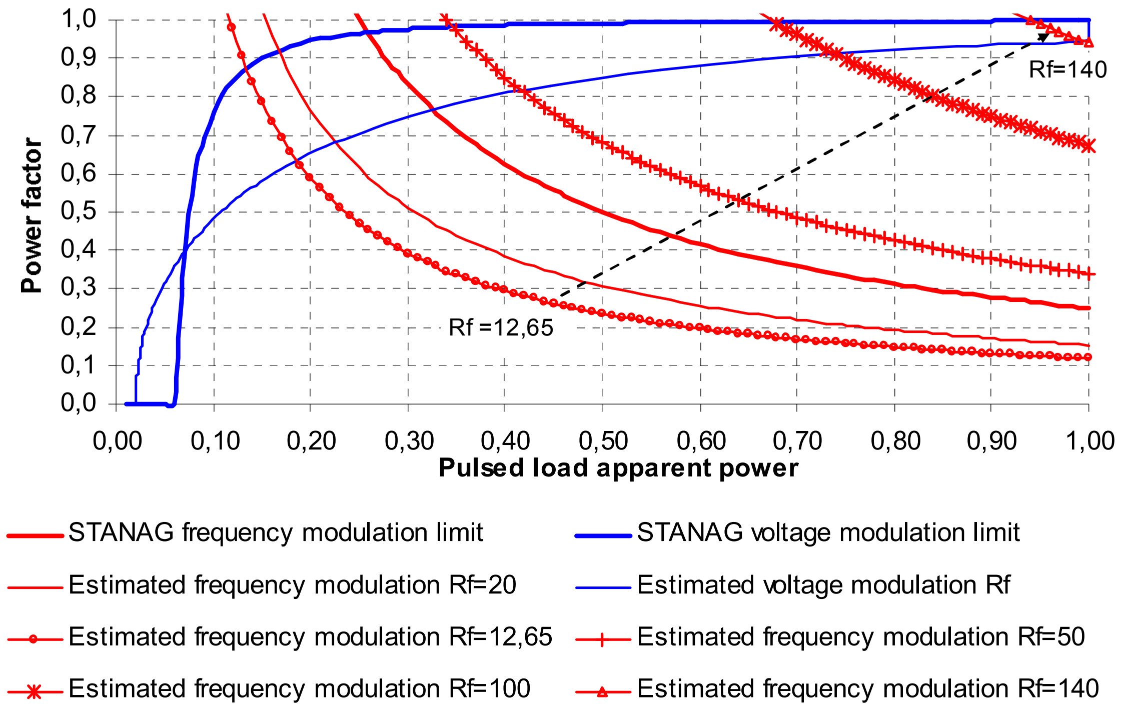

FIGURE 13. Power factor vs pulse load apparent power of the frequency modulation and the voltage modulation of the theoretical analysis for different values of the frequency drop of the frequency regulator of the simplified power system of an S frigate (Rf≥12,65).

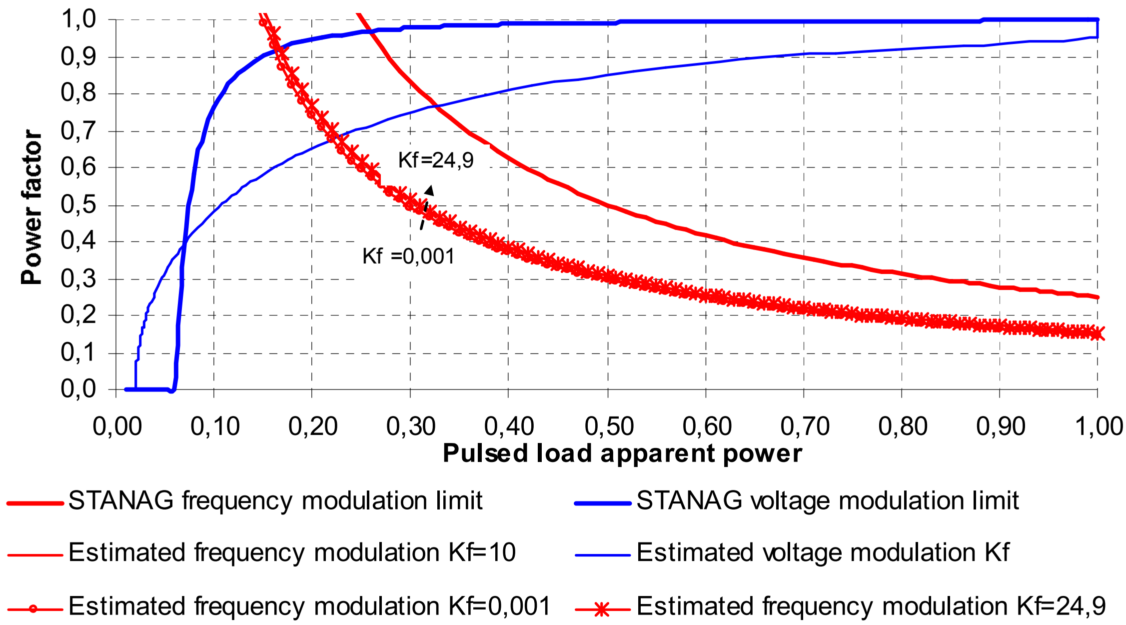

FIGURE 14. Power factor vs pulse load apparent power of the frequency modulation and the voltage modulation of the theoretical analysis for different values of the integral gain of the frequency regulator of the simplified power system of an S frigate (0<Kf<25 Hz).

In Fig. 14, the respective results are presented. The unacceptable operating area due to frequency modulation limit violation decreases extremely slightly, as K_f increases. Practically, the effect of K_f is very limited.

Modulation Limitations for the Simplified Electrical Circuit of a S Frigate Power System: Equivalent Reactance of Cables

The equivalent reactance of the cables X_C affects only voltage modulation. Taking into consideration maximum allowable voltage drop the following analysis has been developed for X_c ranging from 0 up to 0,075 p.u. with a step of 0,005 p.u..

In Fig. 15, the respective results are presented. The unacceptable operating area due to voltage modulation limit violation increases significantly as X_C increases. The unacceptable operating area as obtained by the theoretical analysis is smaller than the respective one of STANAG 1008 for all power factor values if X_C is smaller than 0,035 p.u.. However, if X_C is larger than 0,0385 p.u. then voltage modulation limit would not be satisfied for small pulsed load power factor, as it is obtained by the respective curves.

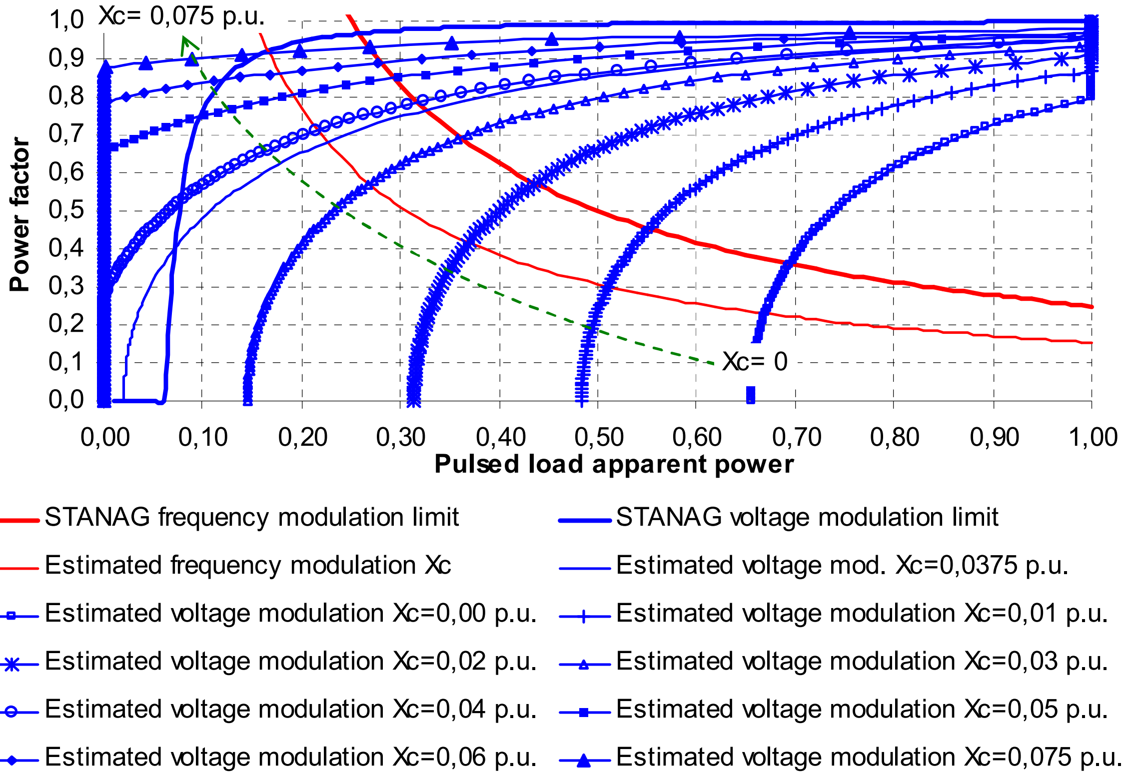

FIGURE 15. Power factor vs pulse load apparent power of the frequency modulation and the voltage modulation of the theoretical analysis for different values of the equivalent reactance of cables of the simplified power system of an S frigate ($0 \leq X_C \leq 0{,}075$ p.u.).

Modulation Limitations for the Simplified Electrical Circuit of a S Frigate Power System: Equivalent Resistance of Cables

The equivalent resistance of the cables, *R,* affects only voltage modulation. Taking into consideration the maximum allowable voltage drop and the proportion between cable reactance and resistance the resistance can be 5 to 1500 times smaller than the respective reactance of usual cable types. Next, the effet of ratio r is investigated, where:

$$r < \frac{X_C}{R} \tag{55}$$

In Fig. 16, the respective results for different values of r are presented. The unacceptable operating area due to voltage modulation limit violation decreases slightly as r increases (cable resistance decreases). However, it should be noted that the critical affecting factor is the cable reactance.

Modulation Limitations for the Simplified Electrical Circuit of a S Frigate Power System: Equivalent Sub-transient Reactance of Generator

The equivalent sub-transient reactance of the generator, X' , affects only voltage modulation. Taking into consideration the practical limitations for the reactance of a synchronous machine it should vary from 9% up to 22% p.u. for turbo-generators, from 12% up to 30% for salient-pole generators with damper winding and from 20% up to 40% for salient-pole generators without damper winding [12]. The respective analysis has been developed for a range of values from 0,09 p.u. up to 0,040 p.u. with a step of 0,01 p.u..

In Fig. 17 the respective results are presented for variable X'. The unacceptable operating area due to voltage modulation limit violation increases slightly as X' increases. The effects of X' are practically limited as it can be calculated and it constitutes a technical characteristic throughout generator lifetime.

Modulation Limitations for the Simplified Electrical Circuit of a S Frigate Power System: Apparent Power of System Base Load without Pulsed Load

The apparent power of system base load S_{L0} affects voltage modulation only. S_{L0} varies from 0 p.u. up to 1 p.u. theoretically, although in a power system of two generators S_{L0} is limited to 0,5 p.u., so that, if one generator is shut down the other generator can take over all the remaining load. Here, the respective analysis has been developed for S_{L0} ranging from 0,00 p.u. up to 1,00 p.u. with a step of 0,01 p.u.. In Fig. 18, the respective results for different values of system base load apparent power are presented.

The unacceptable operating area due to voltage modulation limit violation increases slightly as S_{L0} increases. This is expected under the assumption the system remains stable and reliable. S_{L0} becomes a crucial affecting factor as it varies during ship power system operation. If S_{L0} is larger than 0,7 p.u. then voltage modulation limitation criterion would not be satisfied for small pulsed load power factor values according to the obtained limitation curves.

Modulation Limitations for the Simplified Electrical Circuit of a S Frigate Power System: Proportional Gain of Automatic Voltage Regulator of Generator

The proportional gain of generator automatic voltage regulator, K, affects only voltage modulation. Theoretically, K could take any positive value; however it can not be arbitrarily large as the ratio K/K_V should be small enough to ensure fast response of the Proportional-Integral Controller (PID).

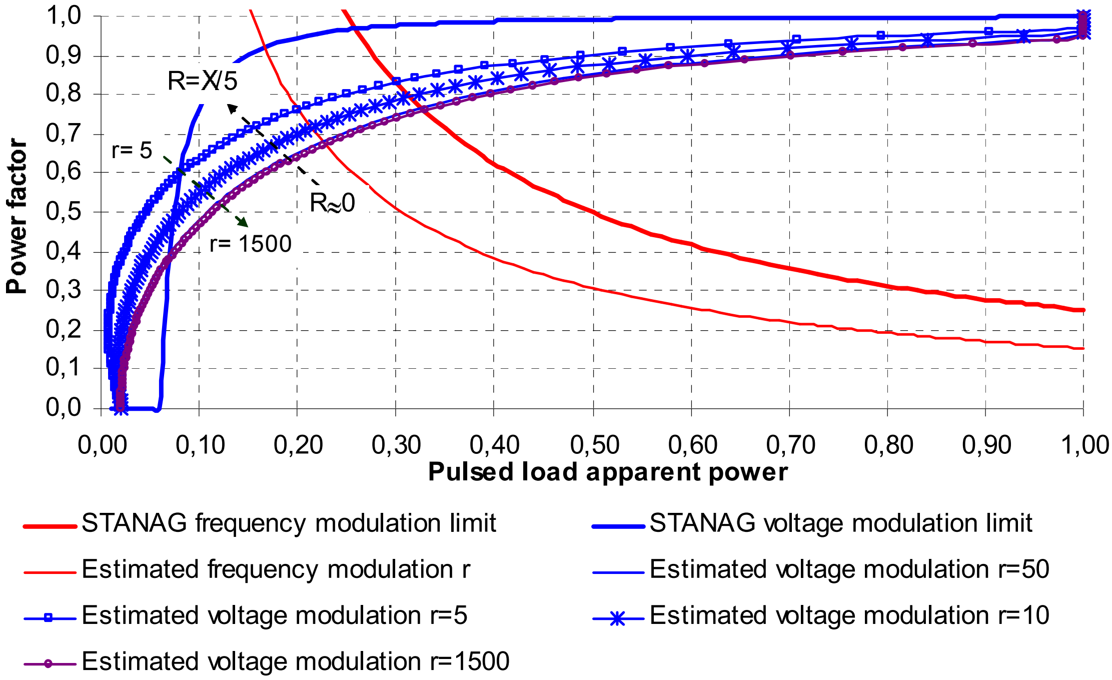

FIGURE 16. Power factor vs pulse load apparent power of the frequency modulation and the voltage modulation of the theoretical analysis for different values of the respective ratio between equivalent reactance to equivalent resistance of cables of the simplified power system of an S frigate ($5 \leq r \leq 1500$).

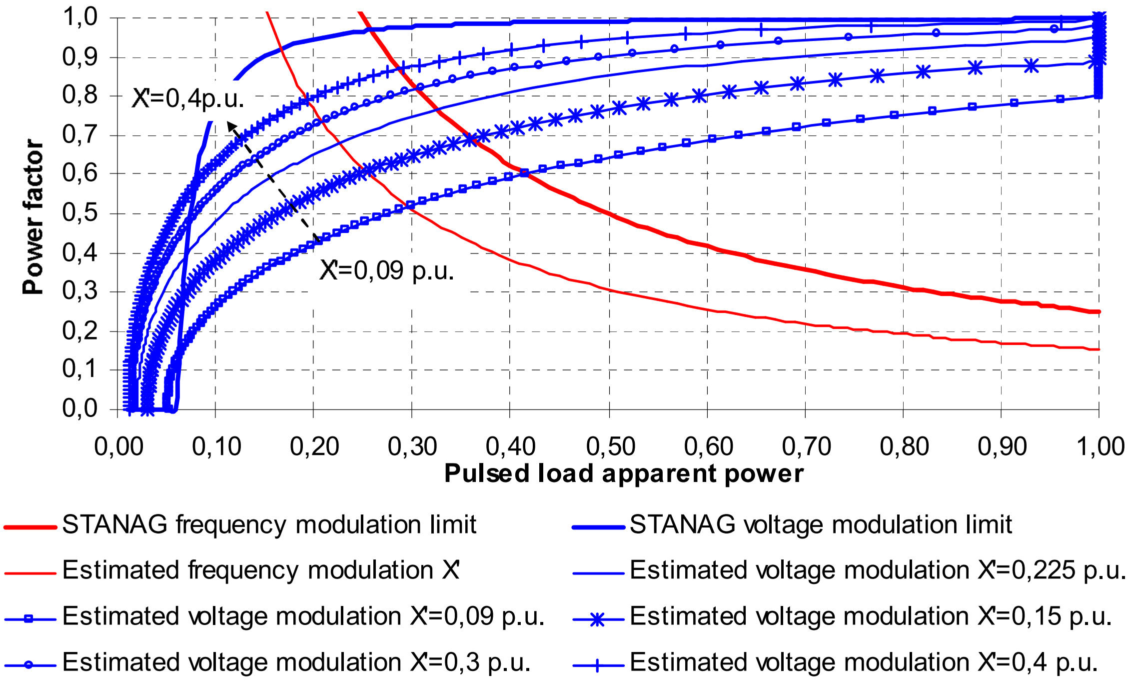

FIGURE 17. Power factor vs pulse load apparent power of the frequency modulation and the voltage modulation of the theoretical analysis for different values of the equivalent sub-transient reactance of generator of the simplified power system of an S frigate (0,09 p.u. $\leq X' \leq$ 0,40 p.u.).

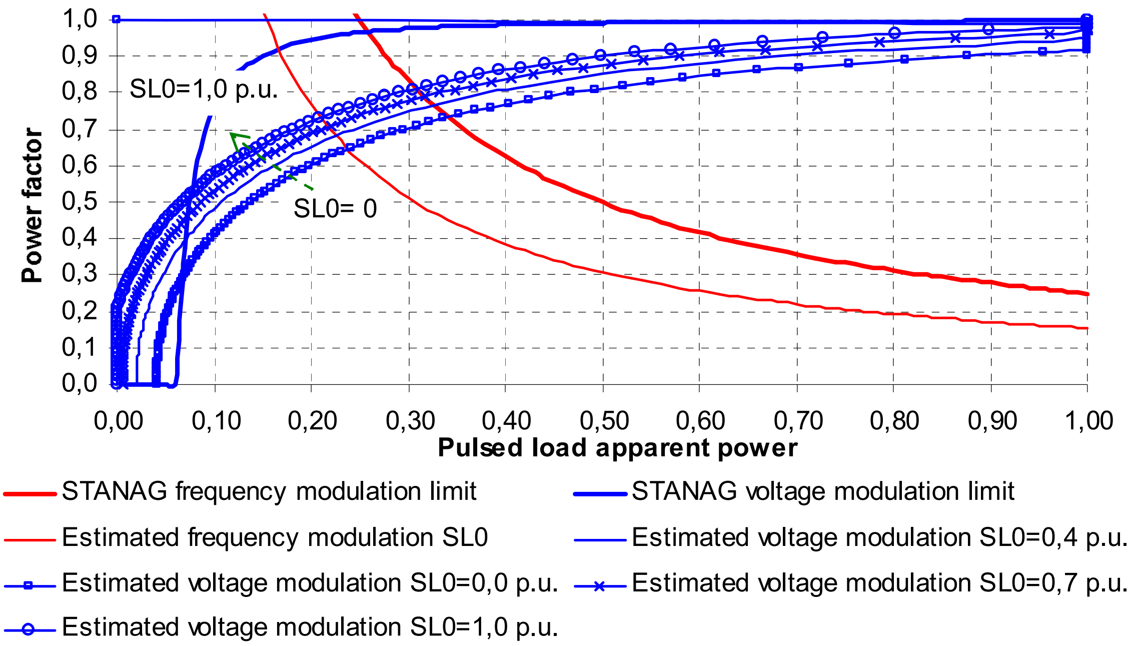

FIGURE 18. Power factor vs pulse load apparent power of the frequency modulation and the voltage modulation of the theoretical analysis for different values of the apparent power of the system base load of the simplified power system of an S frigate (0,00 p.u. ≤ S_{L0} ≤ 1,00 p.u.).

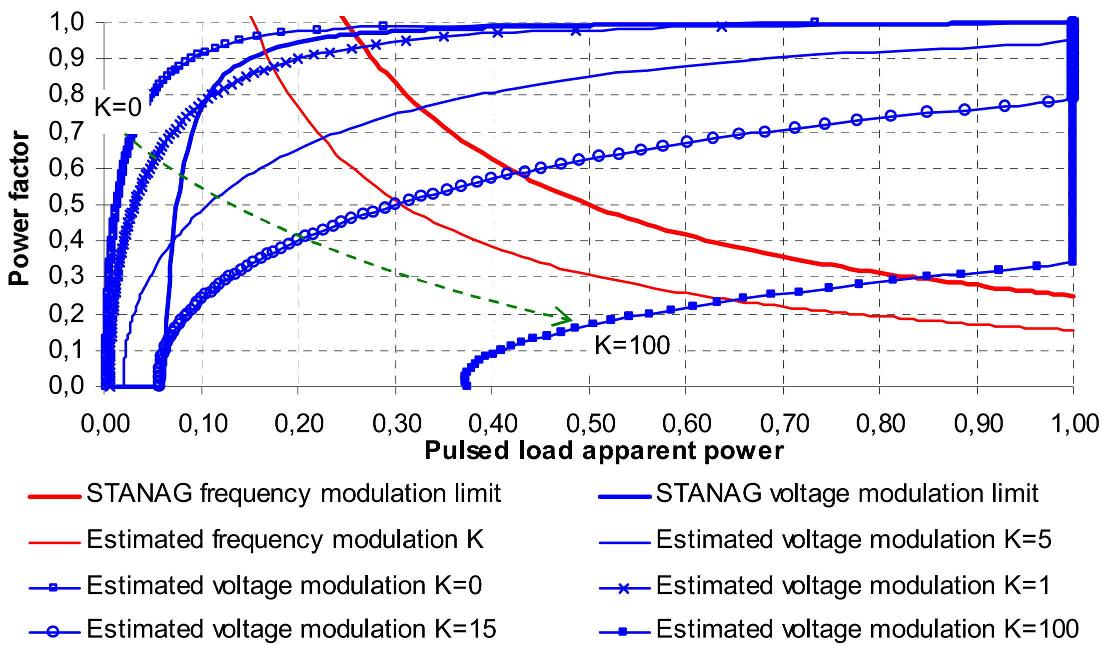

FIGURE 19. Power factor vs pulse load apparent power of the frequency modulation and the voltage modulation of the theoretical analysis for different values of the proportional gain of the automatic voltage regulator of the simplified power system of an S frigate.

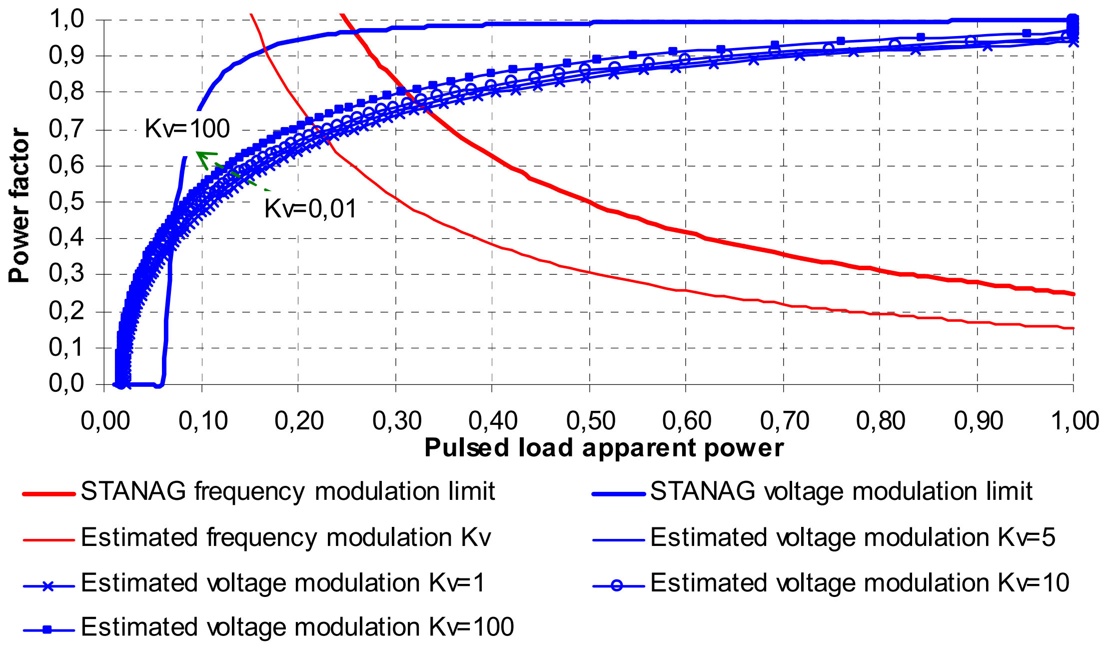

FIGURE 20. Power factor vs pulse load apparent power of the frequency modulation and the voltage modulation of the theoretical analysis for different values of the integral gain of the automatic voltage regulator of the simplified power system of an S frigate.

Here, the following analysis has been developed for K ranging from 0 up to 100 with a step of 1. In Fig. 19, the results for different values of K are presented. The unacceptable operating area due to voltage modulation decreases fast and in a nonlinear fashion as K increases. If K is larger than 16 then STANAG's voltage modulation constraint is satisfied for any pulsed load.

Modulation Limitations for the Simplified Electrical Circuit of a S Frigate Power System: Integral Gain of Automatic Voltage Regulator of Generator

The integral gain K_V of generator automatic voltage regulator affects only voltage modulation. Theoretically, K_V could take any positive value; however as noted above the response time of the PID Controller depends on the ratio K/K_V. Here, the following analysis has been developed for K_V ranging from 0 up to 100, as following: from 0,01 up to 2 with a step of 0,01 and from 2 up to 100 with a step of 1.

In Fig. 20, the respective results for different values of K_V are presented. The unacceptable operating area due to voltage modulation limit violation increases slightly and in a nonlinear fashion as K_V increases. K_V should be positive as for zero value a non-zero voltage "steady-state" error would occur. It should also be large enough in order to obtain large K/K_V ratio, ensuring, in this way, fast response of PID controller.

The proper selection of the values of the PID controller parameters is a complex issue higly related with the dynamics of the of the power system and the generator itself.

CONCLUSIONS

In this paper, STANAG 1008 design constraints for frequency and voltage modulation have been examined applying the proper theoretical analysis in a simplified ship power system. The effects of several parameters such as pulsed load period and duty cycle, the technical characteristics of the generators and their frequency and voltage controllers, the technical characteristics of the cables connecting the pulsed load and generator etc, were examined. The conclusions drawn by the above analysis regarding the significance of the consequent effects are synoptically presented in Table 1.

TABLE (1). Significance of the effects of various parameters and STANAG shortcomings in the frequency/voltage modulation for the simplified ship power system.

Modulation	**Frequency**		**Voltage**	
Parameter	**Significance**	**STANAG shortcoming**	**Significance**	**STANAG shortcoming**
Pulsed load period	Very significant	Yes	Average	Yes (cosφ<0,5)
Pulsed load duty cycle	Very significant	Yes	Significant	Yes (cosφ<0,5)
Generator rotor inertia constant	Average	~	No	-
Frequency drop of frequency regulator	Very significant	Yes (R_f<36)	No	-
Integral gain of frequency regulator	Extremely small	Yes, special cases (K_f=0, etc.)	No	-
Equivalent reactance of cables	No	-	Extremely significant	Yes
Equivalent resistance of cables	No	-	Average	~
Equivalent sub-transient reactance of the generator	No	-	Significant	Yes
Apparent power of system base load without pulsed load	No	-	Significant	Yes
Proportional gain of the automatic voltage regulator	No	-	Very significant	Yes
Integral gain of the automatic voltage regulator	No	-	Small	~

In more detail, the effect of each studied parameter is analyzed next:

- **Pulsed load period, *T*:** It affects significantly frequency modulation, as the unacceptable operating area varies non-monotonically within the region of values studied, [1 ms, 10 s], with a critical value of *T* being being equal to 1,5s for the case studied (see Fig. 10). Voltage modulation practicaly is not affected.
- **Pulsed load duty cycle, *d.c.*:** It affects significantly frequency modulation, as the unacceptable operating area varies non-monotonically within the region of values studied, [0%, 100%], with a critical value of d.c. lying between 65%~70% (see Fig. 11). It also affects voltage modulation but not to the extent in case of frequency modulation.
- **Generator rotor inertia constant, *J'*:** It affects frequency modulation to a limited extent for practical values. This parameter could not be a design variable as it is a technical characteristic of generators.
- **Freqeuncy drop of frequency regulator, R_f:** It affects frequency modulation. Especially, for small values of R_f the effect becomes very significant as the

unacceptable operating area increases considerably. Large values can be chosen for R_f while power system stability issues should be taken into consideration.

- **Integral gain of frequency regulator, K_f:** It affects frequency modulation to a limited extent as this parameter is determined mainly by the other parameters of the generator: rotor inertia *J'* and frequency droop, R_f.
- **Equivalent reactance of cables, X_c:** It affects only voltage modulation. The respective effect becomes extremely significant, as the increase of this parameter enlarges the unacceptable operating area. X_c could vary into a wide range of values, as it depends on the connection point of the different electric consumers and the equivalent reactance of each consumer which varies with time.
- **Equivalent resistance of cables, *R*:** It affects voltage modulation to a limited extent, as it is usually equal to 1/100 up to 1/50 of the respective cable reactance. Its effect is rather degraded by cable reactance effect.
- **Sub-transient reactance of generators, *X'*:** It affects voltage modulation to a significant extent as the increase of *X'* enlarges the unacceptable operating area. This parameter could not be a design variable as it is a technical characteristic of the generators.
- **System base load apparent power, S_{L0}:** It affects voltage modulation to a significant extent as the increase of S_{L0} enlarges the unacceptable operating area in a nonlinear and monotonical fashion. It varies significantly with time as it depends on the variation of the demand of the electric consumers.
- **Proportional gain of equivalent generator automatic voltage regulator, *K*:** It affects voltage modulation to a significant extent as the increase of *K* reduces considerably the unacceptable operating area. This parameter is a technical characteristic of generator controller.
- **Integral gain of generator automatic voltage regulator, K_v:** It affects voltage modulation to a rather limited extent. This parameter is a technical characteristic of generator controller and its value is selected taking into consideration the technical characteristics of the generators, voltage variation limit and the controller response.

The above analysis has proved that the *S-cosf* limitation curve proposed in STANAG 1008 is not unique. Furthermore, it is observed that the examined parameters of the power system model display in a non-linear fashion the *S-cosf* limitation curve. Under these circumstances it seems necessary that the aforementioned parameters (Table 1) affecting voltage and frequency modulation should be taken into consideration in future standards dealing with power quality issues in ship electric power systems.

The theoretical analysis which has been synoptically presented above aims to provide an answer to this problem. Alternatively, the whole power system should be simulated for different operation conditions so that the respective limits for frequency/voltage modulation be obtained. The presented work aims to be the motivation for further research on the topic and to provide general directions to follow for ship electric systems design issues dealing with pulse load integration.

REFERENCES

1. IEEE Std 45-1998, “IEEE Recommended Practice for Electrical Installations on Shipboard”.
2. STANAG 1008, “Characteristics of Shipboard Electrical Power Systems in Warships of the NATO Navies”, NATO, Edition 9, 24 Aug. 2004.
3. USA MIL-STD-1399(NAVY), “Interface standard for Shipboard systems – Section 300A – Electric Power, Alternating Current”.

4. Howard A., Smolleck Satish J., Ranade Nadipuram R., Prasad Rudolph, O. Velasco, “Effects of Pulsed – Power Loads upon an Electric Power Grid”, IEEE/PSS 1990 Sumner meeting, Minneapolis, Minnesota, July 15-19, 1990.
5. F.D. Kanellos, I.K. Hatzilau, J. Prousalidis, E. Styvaktakis, “Simulation of a Shipboard Electrical Network (AES) comprising Pulsed Loads”, Engine as a Weapon II, IMarEST, Dec. 2006, London.
6. F.D. Kanellos, I.K. Hatzilau, J. Prousalidis, “Investigation of voltage/frequency modulation in ship electric networks with pulsed loads according to STANAG 1008 design constraints”, All Electric Ship Conference 2007, London.
7. G. J. Tsekouras, F.D.Kanellos, J.M. Prousalidis, I.K. Hatzilau, “STANAG 1008 design constraints for pulsed loads in the frame of the All Electrical Ships”, Nausivios Chora, A journal in Naval Sciences and Technology, vol. 3, 2010, pp. 115-154.
8. F.D.Kanellos, G. J. Tsekouras, J. Prousalidis, I.K. Hatzilau, “An effort to formulate frequency modulation constraints in Ship-Electrical Systems with Pulsed Loads”, IET Electrical Systems in Transportation, vol. 1, issue 1, 2011, pp. 11-23.
9. F.D.Kanellos, G. J. Tsekouras, J. Prousalidis, I.K. Hatzilau, “Effort to formulate voltage modulation constraints in ship-electrical systems with pulsed loads”, IET Electrical Systems in Transportation, vol. 2, issue 1, 2012, pp. 18-28.
10. P. Krause, “Analysis of Electric Machinery”, McGraw-Hill, 1986.
11. Chee-Mun Ong, “Dynamic Simulation of Electric Machinery using Matlab/Simulink”, Prentice Hall PTR, 1998.
12. H. Gremmel, G. Kopatsch. “Switchgear Manual”, ABB AG Germany, 11th edition, 2008.